Supporting Information

Effect of Pd and Au on Hydrogen Abstraction and C-C Cleavage in Photo-conversion of Glycerol: Beyond Charge Separation

*Dongdong Lv,[#ac] Yechen Lei,[#bc] Dongsheng Zhang,[d] Xin Song,[c] Yong-Wang Li,[c] J. W. (Hans) Niemantsverdriet,[ce] Weichang Hao,[*a] Yonghong Deng,[*b] Ren Su[*cd]*

[a] School of Physics and BUAA-UOW Joint Research Centre, Beihang University, Beijing 100191, China.

[b] Department of Materials Science & Engineering, Southern University of Science and Technology (SUSTech), Shenzhen 518055, P. R. China

[c] SynCat@Beijing, Synfuels China Technology Co. Ltd., Leyuan South Street II, No.1, Yanqi Economic Development Zone C#, Huairou District, Beijing, 101407, China.

[d] Soochow Institute for Energy and Materials InnovationS (SIEMIS), Key Laboratory of Advanced Carbon Materials and Wearable Energy Technologies of Jiangsu Province, Soochow University, Suzhou, P. R. China

[e] SynCat@DIFFER, Syngaschem BV, 6336 HH Eindhoven, The Netherlands.

Corresponding Authors

* suren@suda.edu.cn (R. Su); dengyh@sustc.edu.cn (Y. Deng); whao@buaa.edu.cn (W. Hao)

1 Photocatalytic process analysis

The gas phase and liquid phase products evolved during photocatalytic glycerol conversion under deaerated conditions were determined by *in-situ* mass-spectrometry (MS) and nuclear magnetic resonance (NMR), respectively.

MS analysis: Glycerol oxidation was carried out in 1 atm Ar condition. The mass spectrometer (MS, HHPR-20, Hiden) was used to record gas phase products (Figure S1). A powder sample (50 mg) was dissolved in 3 mL of water and sonicated for 1 min. Then the suspension was dropped on a glass reactor and dried at 50 ^{o}C for 1 h to prepare the sample film. A 7 μL of glycerol-water solution was dosed on the sample film (glycerol: water = 5:1, 0.08 mmol), which was loaded into MS reactor (dead volume of 110 mL). The reactor was then sealed, and the leakage of the system was checked. The photodissociation of glycerol was evaluated under low pO_2 (< 200 ppm) and the control of initial O_2 concentration was realized using Ar gas exchange. A UV LED light (365 nm, 500 mW) was used as light source.

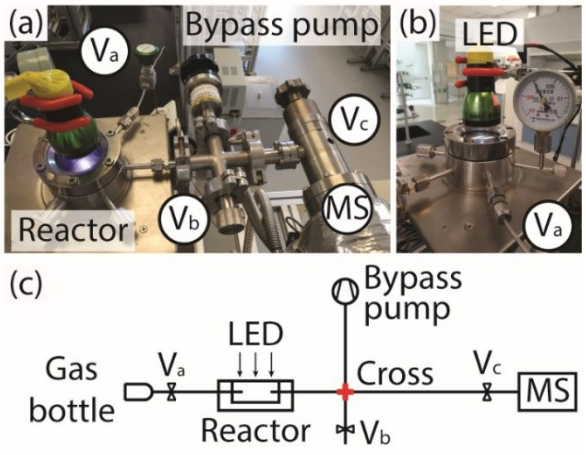

Figure S1. (a) and (b) Photos of *in-situ* MS reaction system and reactor cell; (c) Scheme of the *in-situ* MS reaction system. V_a - V_c are gas-inlet valve, vent valve and leak valve, respectively.

1) **Stabilization of MS and photocatalytic glycerol oxidation reaction:** The mass spectrometer was turned on prior to the experiment with the MS chamber pressure set to 1 e^{-7} mbar under 1 bar air pressure by adjusting the leak-valve. The pO_2 and pN_2 were stabilized at ~1 e^{-9} and ~4 e^{-9} mbar for all experiments, respectively. After Ar gas exchange, pO_2 decreases to ~5 e^{-12} mbar prior to irradiation and the signals of all gases are stable.

2) **Data processing protocols:** the data processing procedures have been described previously in detail.[1] In short, the sum of pN_2 and pO_2 recorded in air was used to correlate the measured pressures of the evolved gases in the vacuum chamber of the MS to the real pressure of the reactor cell. The quantity of evolved gases thus can be calculated by the following equation:

$$n(gas) = p(gas)_{Reactor} * V_{Reactor} / RT \quad \text{Eq. (1)}$$

$$p(gas)_{Reactor} = RSF(gas) * p(gas)_{Det} * p(Air)_{Reactor} / p(Air)_{Det} \quad \text{Eq. (2)}$$

where,

$p(gas)_{Reactor}$ is the partial pressure of a specific gas in the Reactor cell;

$p(gas)_{Det}$ is the partial pressure of a specific gas measured by the mass spectrometer;

$p(Air)_{Reactor}$ is the pressure of air in the Reactor cell (100 kPa);

$p(Air)_{Det}$ is the pressure of air detected by the mass spectrometer;

$V_{Reactor}$ is the volume of the Reactor cell and all connected tubing (the volume is 110 mL);

RSF (gas) is the relative sensitivity factor of a specific gas (0.284 for H_2, 1.4 for CO_2, 0.86 for O_2, 0.9 for H_2O, 1.05 for CO and 1 for CH_2O).

NMR data analysis: After the photocatalytic reaction, the liquid products were collected and analyzed using H-NMR. D_2O (0.5 mL) was dropped in the reactor and the liquid product was collected by centrifuging from suspension after the reaction was completed. Then 10 μL of maleic

acid solution (1 mM) was added into the solution, which was used as reference to determine the conversion of glycerol. The conversion of glycerol was calculated as follows:

$$Conversion/\% = \frac{N_{total} - n_{remain}}{N_{total}} \quad \text{Eq. (3)}$$

where

N_{total} is the molar amount of glycerol added into the reactor;

n_{remain} is the molar amount of glycerol after the reaction;

Estimation of quantum efficiency: The apparent quantum efficiency (AQE) was estimated as the following according to Eq. (4):

$$AQE = 2n(H_2)_t \cdot N_A / (N_{photon}) \quad \text{Eq. (4)}$$

where, $n(H_2)_t$ is the number of moles of hydrogen evolved within 24 hours (280 μmol for Pd/TiO_2 and 120 μmol for Au/TiO_2);

N_A is the Avogadro's number (6.02×10^{23} mol^{-1});

N_{photon} is the number of incident photon within 24 hours (2.4×10^{22}); (The light intensity is 150 mW and the wavelength of LED lamps is 365 nm)

We find the AQEs for Pd/TiO_2 and Au/TiO_2 are 1.4% and 0.6%, respectively.

2 Reaction mechanism analysis

In-situ **FTIR-MS:** The glycerol photo-dissociation was investigated by *in-situ* Fourier transform infrared (FTIR) spectrometer (Vertex 70, Bruker) coupled with a mass spectrometer (MS, HPR-20, Hiden analytics), which allowed us to probe the evolution of reactant, the intermediates and the products both in the surface and gas phase. As shown in Figure S2 (a)-(b),

the FTIR and MS were connected *via* a multi reflection attenuated total reflection (ATR) flow cell (Harrick). Prior to each experiment, the photocatalyst materials were deposited on the Ge window of the ATR cell (Figure S2c). The schematic drawing of the apparatus was also shown in Figure S2 (d).

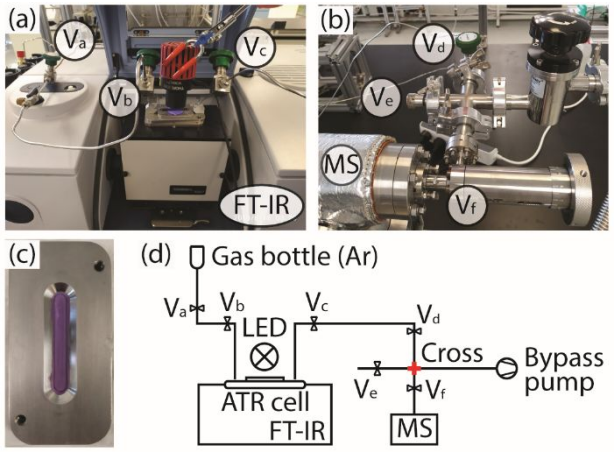

Figure S2. (a) and (b) Photos of the *in-situ* FTIR-MS, (c) the ATR cell with the sample (Au/TiO_2) deposited on the Ge window. (d) Sketch of the *in-situ* FTIR-MS apparatus. V_b – V_f are gas inlet and outlet valves, mass inlet valve, vent valve, leak valve, respectively.

Details of the in-situ FTIR-MS setup are described in the following:

1) **Deposition of the photocatalyst on the Ge window.** A 20 mg of the photocatalyst was added into 2 ml of DI water and sonicated for 1 min. Then 1 ml of the suspension was dropped on the clean Ge window that is sealed in the bottom part of the ATR cell. The cell was dried at 45 ^{o}C for 1 h to evaporate the water and kept at RT for 1 h before ATR cell assembly.

2) **ATR cell assembly and connection with MS.** The bottom part of the ATR cell with catalyst film on the Ge window was sealed with the top part of the ATR cell with a quartz window. Two 1/8-inch tubing provided the connection with the Ar gas bottle and the MS, respectively. One

tubing was connected to the gas bottle *via* a high vacuum valve (V_b) and a reduction valve (V_a), whereas the other tubing was connected to the MS *via* a high vacuum valve (V_c) and a leak valve (V_f). A 4-way cross was inserted in between the V_c and V_f for MS inletting and venting purposes *via* two high vacuum valves (V_d and V_e). The ATR cell and all connected tubing were leak-tight, which allow us performing reactions under vacuum conditions.

Experimental protocols:

1) **Stabilization of the mass spectrometer (MS):** The stabilization of the MS is the same as described above.

2) **Baseline of FTIR.** An IR spectrum of the photocatalyst film deposited on the Ge window was measured in Ar gas and set as baseline. Prior to the measurement, the ATR cell was purged by Ar for 10 min and evacuated using a bypass pump to remove surface adsorbed water.

3) **Dosing glycerol and initiate photocatalytic reaction**. The ATR cell was disassembled after recording baseline to dose 2 μL of glycerol using a 10 μL micro syringe. The ATR cell was then reassembled and purged with Ar for 10 min to remove trace amount of water. Meanwhile, the O_2 partial pressure was reduced to < $5e^{-12}$ mbar. V_b and V_e were closed and the cell was kept in dark to check the leakage and stable gas signal. The IR spectra were recorded every 5 min until the glycerol signals were stabilized. Finally, the UV irradiation was commenced using a 365 nm LED (Optimax-365, Spectroline). The LED light source was placed on top of the quartz window, and a steady light intensity (130 mW) was realized by using a DC power supply.

Data processing protocols:

1) **MS:** The calculation process is identical as described above. Here the volume of ATR reactor is 55 mL.

2) **FTIR.** All IR spectra were recorded from 4000 cm^{-1} to 650 cm^{-1}, and each spectrum was scanned for 32 times to yield a high signal-to-noise ratio. The hydroxyl peak (ν[OH] ~ 3200 cm^{-1}), C-H bond (ν[CH] ~ 3000-2750 cm^{-1}) peak,[2-3] C=O peak (ν[C=O]=1717 cm^{-1})[4] and carbon monoxide (ν[CO]=1916 cm^{-1})[5] were integrated to calculate the evolution kinetics, respectively.

3 XPS analysis

A 3 mg of each catalyst was deposited on the XPS sample stage, which was then irradiated by an UV lamp for 2 h to clean the catalyst surface. Then 0.2 μL of glycerol solution was dosed onto the surface of the catalyst, which was then analyzed by XPS. After the analysis was completed, the sample was transferred from the analysis chamber to the load-lock for UV irradiation. Subsequently, the sample was transferred back to the analysis chamber for XPS analysis.

4 Results and discussion

The metal loading of modified TiO_2 determined by ICP is shown in Tablet S1.

Table S1. metal loading of the synthesized catalysts

Sample	Pd / wt%	Au / wt%
1 wt%Pd/TiO_2	0.88	-
1 wt%Au/TiO_2	-	0.76

X-ray diffraction (XRD) analysis of pristine TiO_2 (Degussa P25) and metal decorated TiO_2 are shown in Figure S3. Both Au/TiO_2 and Pd/TiO_2 exhibit similar diffraction patterns to that of the pristine TiO_2, suggesting the photodeposition process has little effect on the TiO_2. The metal (Au and Pd) diffraction peaks are not detected because of the low loading (1 wt%).

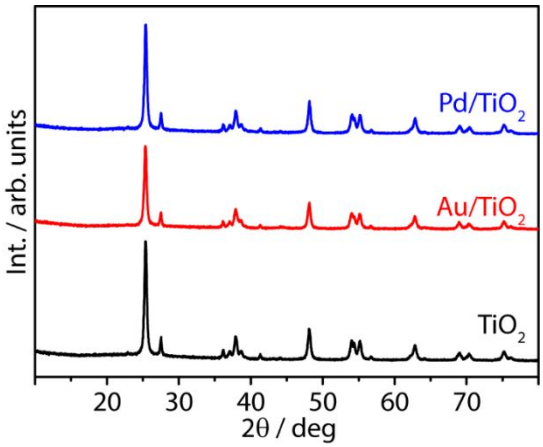

Figure S3. XRD patterns of pristine TiO_2, 1 wt% Au/TiO_2 and Pd/TiO_2, respectively

Figure S4 shows the XPS spectroscopy recorded using K-Alpha (Thermo-Scientific) with an Al Kα radiation source. Only Ti, O, C and the corresponding metal (Au and Pd) are detected from the survey spectra, which indicates the purity of the samples (Figure S4a). The C1s spectra of all samples can be deconvoluted into two peaks (Figure S4b), which can be assigned to the C-O bond and C-C bond (284.8 eV). We use C-C bond of C1s as calibration reference. No peak shift is observed for both Ti2p and O1s, regardless of the TiO_2 samples.

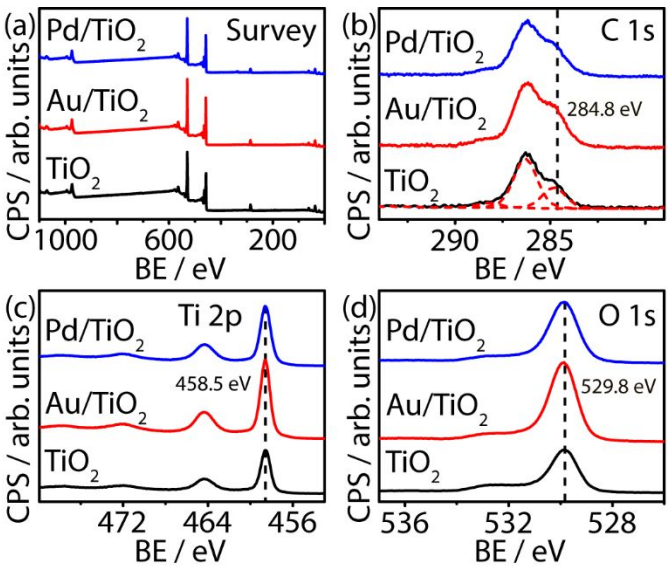

Figure S4. (a) XPS survey spectra of pristine TiO_2 and metal (1 wt% Au and Pd) loaded TiO_2; and XPS spectra of (b) C 1s, (c) Ti 2p and (d) O 1s of the corresponding samples.

Figure S5 shows the time-resolved mass spectra recorded during reaction. As shown in **region I**, the signals of all gases are stabilized in atmosphere for 2 hours. Prior to photocatalytic reaction, the air in the chamber is exchanged by evacuation and Ar purging, and all signals are stabilized for 1 hour under 1 bar Ar. **Region II** displays the evolution of all gas-phase products upon irradiation. All signals are stabilized after the light was switched off, as shown in **region III**.

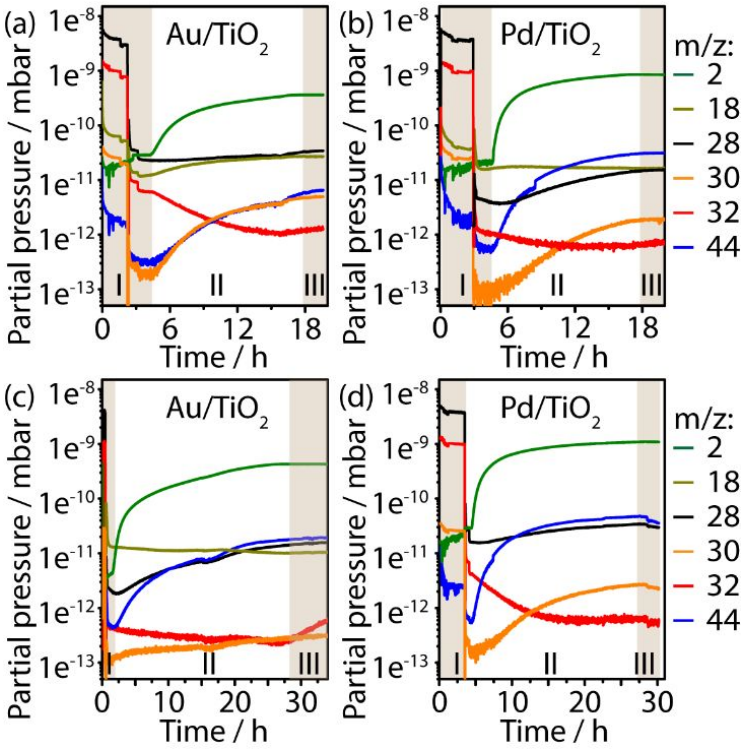

Figure S5. Time-resolved mass spectra during the phtocatalytic glycerol oxidation. The m/z of 28, 32, 44, 18, 2 and 30 are CO, O_2, CO_2, H_2O, H_2 and formaldehyde (CH_2O). The three region represent (I) stable signal prior to experiments, (II) photocatalytic reaction under irradiation, (III) stable signal after light is off. (a) and (b) the irradiation time is 12 h; (c) and (d) the irradiation time is 24 h.

The NMR spectra of extracted products after photocatalytic glycerol conversion are shown in Figure S6. The major products are glycolaldehyde, formic acid, and 1,3-dihydroxyacetone.

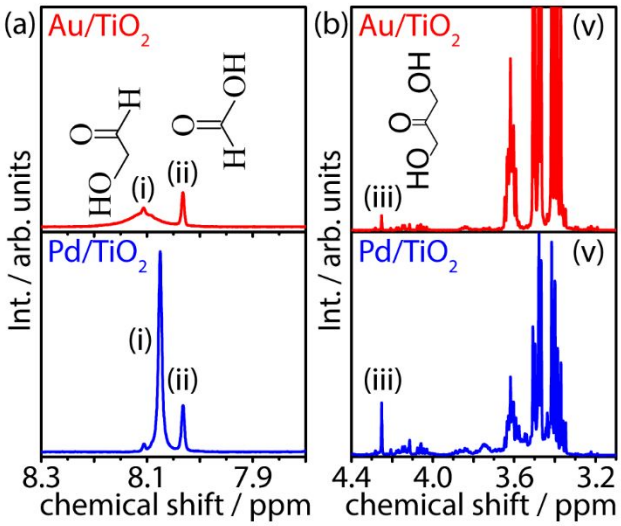

Figure S6. NMR analysis of photocatalytic glycerol conversion products using Au and Pd decorated TiO_2 under deaerated conditions. (a) and (b) irradiated for 12 h. (i, ii, iii and v are assigned to glycolaldehyde, formic acid, 1,3-dihydroxyacetone and glycerol)

Figure S7(a) and 7(b) show the *in-situ* FT-IR recorded during photocatalytic glycerol conversion by Au and Pd modified TiO_2. The evolution of integrated ν(CH) and ν(CO) peaks is shown in Fig. S7(c) and 7(d).

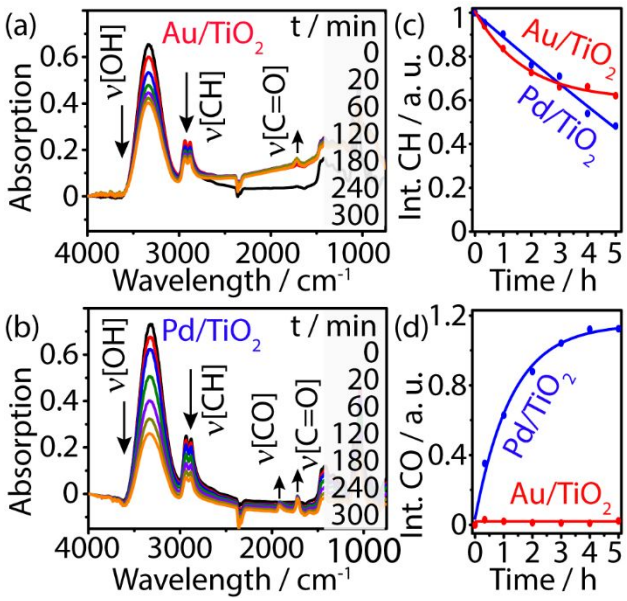

Figure S7. (a) and (b) Liquid-phase products evolution over Au/TiO_2 and Pd/TiO_2 recorded using *in-situ* FTIR-MS during photocatalytic glycerol conversion under deaerated conditions. (c) and (d) Evolution of integrated CH and CO vibrational peaks as a function of irradiation time (ν_{as}(CH) = 2934 cm^{-1} and ν_s(CH) = 2879 cm^{-1}, ν(CO) = 1916 cm^{-1} and ν(C=O) = 1717 cm^{-1}).

Figure S8 shows the *in-situ* FT-IR recorded during photocatalytic dissociation of paraformaldehyde by Au and Pd modified TiO_2.

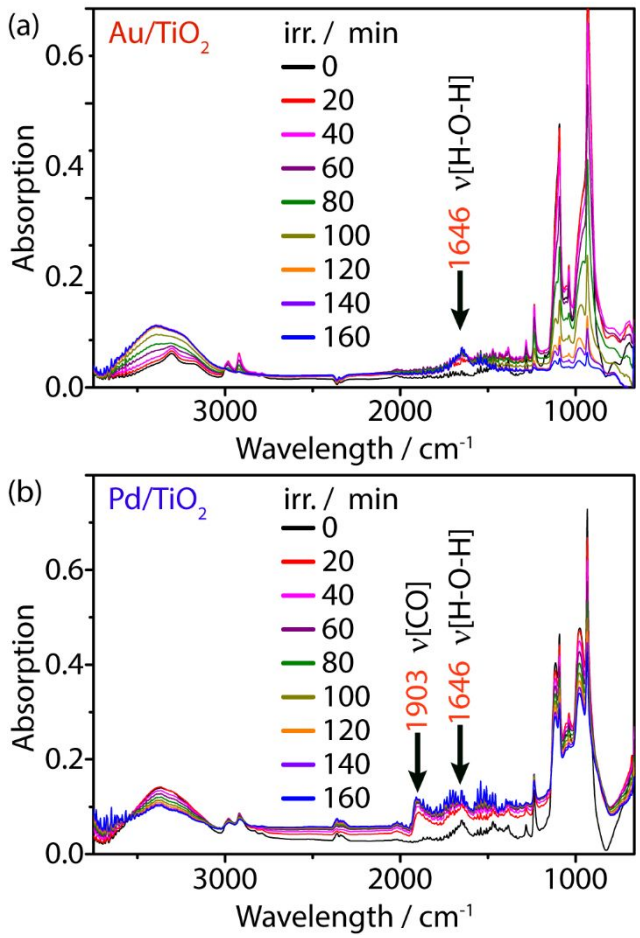

Figure S8. Liquid phase products during photocatalytic dissociation of paraformaldehyde under deaerated condition determined by *in-situ* FTIR-MS over (a) Au/TiO_2 and (b) Pd/TiO_2, respectively.

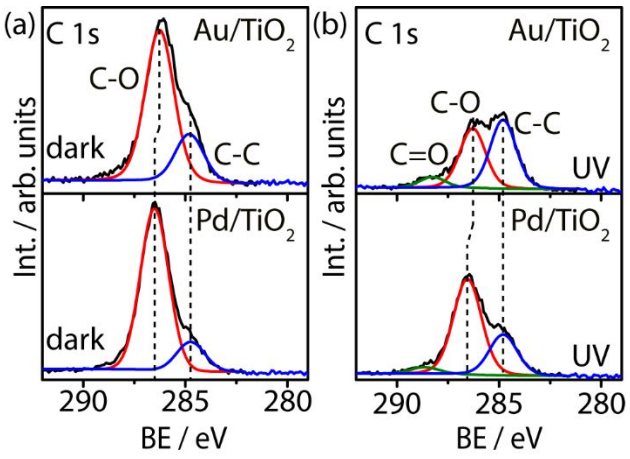

Figure S9. XPS spectra of C 1s for Au/TiO_2 and Pd/TiO_2 (a) before and (b) after photocatalytic glycerol conversion under deaerated conditions.

References

(1) Jin, X.; Li, C.; Xu, C.; Guan, D.; Cheruvathur, A.; Wang, Y.; Xu, J.; Wei, D.; Xiang, H.; Niemantsverdriet, J.; *et al.* Photocatalytic C-C Bond Cleavage in Ethylene Glycol on TiO_2: A Molecular Level Picture and the Effect of Metal Nanoparticles. *J. Catal.* **2017**, *354*, 37-45.

(2) Nguyen, T. T.; Raupach, M.; Janik, L. J., Fourier-Transform Infrared Study of Ethylene Glycol Monoethyl Ether Adsorbed on Montmorillonite: Implications for Surface Area Measurements of Clays. *Clays Clay Miner.* **1987**, *35*, 60-67.

(3) Valerio, O.; Horvath, T.; Pond, C.; Manjusri, M.; Mohanty, A., Improved Utilization of Crude Glycerol from Biodiesel Industries: Synthesis and Characterization of Sustainable Biobased Polyesters. *Ind. Crop. Prod.* **2015**, *78*, 141-147.

(4) Busca, G.; Lamotte, J.; Lavalley, J. C.; Lorenzelli, V., Ft-Ir Study of the Adsorption and Transformation of Formaldehyde on Oxide Surfaces. *J. Am. Chem. Soc.* **1987**, *109*, 5197-5202.

(5) Ivanova, E.; Mihaylov, M.; Thibault-Starzyk, F.; Daturi, M.; Hadjiivanov, K., Ftir Spectroscopy Study of Co and No Adsorption and Co-Adsorption on Pt/TiO_2. *J. Mol. Catal. A* **2007**, *274*, 179-184.